



OPEN

New localized/delocalized emitting state of Eu^{2+} in orange-emitting hexagonal EuAl_2O_4

SUBJECT AREAS:
NONLINEAR OPTICS
PHOTONIC CRYSTALSFeng Liu^{1,2}, Richard S. Meltzer², Xufan Li¹, John D. Budai³, Yu-Sheng Chen⁴ & Zhengwei Pan^{1,2}Received
12 August 2014Accepted
3 November 2014Published
18 November 2014Correspondence and
requests for materials
should be addressed to
F.L. (fliu@uga.edu) or
Z.W.P. (panz@uga.
edu)¹College of Engineering, University of Georgia, Athens, GA 30602, USA, ²Department of Physics and Astronomy, University of Georgia, Athens, GA 30602, USA, ³Materials Science and Technology Division, Oak Ridge National Laboratory, Oak Ridge, Tennessee 37831, USA, ⁴ChemMatCARS, University of Chicago, Argonne, Illinois 60439, USA.

Eu^{2+} -activated phosphors are being widely used in illuminations and displays. Some of these phosphors feature an extremely broad and red-shifted Eu^{2+} emission band; however, convincing explanation of this phenomenon is lacking. Here we report a new localized/delocalized emitting state of Eu^{2+} ions in a new hexagonal EuAl_2O_4 phosphor whose Eu^{2+} luminescence exhibits a very large bandwidth and an extremely large Stokes shift. At 77 K, two luminescent sites responsible for 550 nm and 645 nm broadband emissions are recognized, while at room temperature only the 645 nm emission band emits. The 645 nm emission exhibits a typical radiative lifetime of 1.27 μs and an unusually large Stokes shift of 0.92 eV. We identify the 645 nm emission as originating from a new type of emitting state whose composition is predominantly that of localized $4f^65d$ character but which also contains a complementary component with delocalized conduction-band-like character. This investigation provides new insights into a unique type of Eu^{2+} luminescence in solids whose emission exhibits both a very large bandwidth and an extremely large Stokes shift.

Eu^{2+} -activated phosphors usually exhibit broadband luminescence under external excitations^{1–3}. Most of these emissions are attributed to the dipole-allowed $4f^65d \rightarrow 4f^7$ transitions associated with relatively large transition probabilities and short radiative lifetimes (0.4–1.8 μs)³. In these phosphors, the emissions from the localized $4f^65d$ states exhibit typical Stokes shifts in the range of 0.1–0.5 eV³.

Besides the normal Eu^{2+} $4f^65d \rightarrow 4f^7$ transitions, some Eu^{2+} -activated phosphors exhibit extraordinarily broad emission bands associated with abnormally long radiative lifetimes (typically $>2 \mu\text{s}$) and extremely large Stokes shift (typically $>0.6 \text{ eV}$)^{4–9}. This type of emission was described as anomalous luminescence by McClure and Pedrini⁴. In their model, the lowest $4f^65d$ states of Eu^{2+} generally lie inside the host conduction band, and the excitation of a Eu^{2+} ion results in its autoionization, followed by trapping of a conduction electron close to the ionized Eu^{2+} ion. As a result, a Eu-trapped exciton becomes the emitting state. The transition between the exciton-like state and the $4f^7$ ground state of Eu^{2+} is forbidden by the dipole selection rule in the anomalous luminescent phosphors⁴; therefore the transition probabilities for both anomalous luminescence and its corresponding excitation are generally small, resulting in a long radiative lifetime and a weak (often undetectable) exciton excitation band. Moreover, in anomalous luminescent phosphors, the delocalization of the lowest excited state (i.e., the exciton-like state) induces the ligand ions around the Eu^{2+} to undergo a considerably larger relaxation than for the normal case of Eu^{2+} , which is reflected in the emission spectrum by an extremely large Stokes shift^{4,6}.

There is also a special class of Eu^{2+} -activated phosphors that exhibit the characteristics of both normal $4f^65d \rightarrow 4f^7$ transitions (e.g., large transition probabilities for emission and excitation) and anomalous luminescence (e.g., very large bandwidth and Stokes shift of emission)^{10–15}. Based on the relationship between the luminescence and host crystalline structure in this special class of Eu^{2+} -activated phosphors, Poort *et al.* attributed this type of emission to $4f^65d \rightarrow 4f^7$ transitions and suggested that the linear chain structure of large cations in the lattice (depending on the values of lattice parameters) contributed to this special luminescence¹⁰. However, with the emergence of more and more novel Eu^{2+} -activated phosphors, in which the chain structure of the large cations is usually absent in the hosts^{11–15}, Poort's explanation is no longer adequate for this special type of broadband emissions.

In this study, we identify and investigate a Eu^{2+} broadband emission associated with both a large transition probability and an extremely large Stokes shift (0.92 eV) in a new concentrated europium aluminate phosphor,



hexagonal EuAl_2O_4 (*h*-EAO). We attribute this unusual emission to the delocalized nature of the excited electrons in the $4f^65d$ emitting level. That is, a ground-state $4f^7$ electron is excited to the lowest $4f^65d$ state, from where the excited electron may delocalize to the host continuum state according to a small probability, followed by radiative emission from the $4f^65d$ state. This investigation provides new insights into a unique type of Eu^{2+} luminescence in solids whose emission exhibits both a very large bandwidth and an extremely large Stokes shift.

Results

Photoluminescence (PL) at room temperature and low temperature. The *h*-EAO phosphor was fabricated by carbothermal reaction and evaporation of a mixture of Eu_2O_3 , Al_2O_3 and graphite powders at 1450°C in a flowing argon environment in a tube furnace system. The detailed fabrication process was described in ref. 16. The carbothermal reaction produced a weakly reducing environment which facilitated the formation of effective Eu^{2+} luminescence centers in the concentrated *h*-EAO phosphor^{16,17}. The *h*-EAO phosphor is nanoribbon-like with typical widths of 200–1000 nm, thicknesses of 50–300 nm, and lengths of 50–500 μm ¹⁶. The *h*-EAO nanoribbons exhibit a hexagonal space lattice with a new set of lattice parameters of $a = b = 6.15 \text{ \AA}$ and $c = 10.57 \text{ \AA}$, as determined by synchrotron X-ray Laue microdiffraction¹⁶ and further confirmed by synchrotron X-ray microcrystallographic measurements (see Supplementary Information, including Supplementary Table 1 and Supplementary Fig. 1, for the determination of the unit cell structure of *h*-EAO). The X-ray microdiffraction results showed that each nanoribbon in the phosphor is a single crystal with composition EuAl_2O_4 , and no evidence was found to suggest the presence of second phases or inclusions embedded in the single crystals. X-ray absorption near edge structure measurement on Eu L_3 edge showed that the Eu ions in *h*-EAO are predominantly in the divalent state, i.e., Eu^{2+} (ref. 16).

Under blue light or ultraviolet excitation, the *h*-EAO phosphor exhibits intense orange emission. Figure 1a shows the normalized PL emission and excitation spectra of *h*-EAO at room temperature, as well as the low-energy side of the diffuse reflectance absorption spectrum. At room temperature, the shapes of the emission and excitation spectra are independent of the corresponding excitation and monitoring wavelengths, respectively (Supplementary Fig. 2a). The emission spectrum contains a Gaussian-shaped emission band peaking at 645 nm ($\sim 1.93 \text{ eV}$) with a full width at half maximum (FWHM) of 0.45 eV. The PL excitation spectrum in Fig. 1a contains two excitation bands: a high-energy band peaking at 365 nm ($\sim 3.40 \text{ eV}$) and a low-energy band peaking at 435 nm ($\sim 2.85 \text{ eV}$). The low-energy 435 nm excitation band starts at $\sim 540 \text{ nm}$ ($\sim 2.3 \text{ eV}$), which coincides with the onset of the diffuse reflectance absorption spectrum and conforms to the “mirror image” of the 645 nm emission band (dashed curve in Fig. 1a), indicating that the 435 nm excitation band corresponds to the lowest excited state in the phosphor. Thus, the Stokes shift of the emission can be determined to be 0.92 eV, which is equal to the energy difference between the intensity maxima in the lowest excitation band and the emission band.

In contrast to the room-temperature luminescence, at 77 K the shapes of the emission and excitation spectra become dependent on their respective excitation and monitoring wavelengths (Fig. 1b). A Gaussian-shaped emission band peaking at 645 nm is obtained under 460 nm excitation; the spectral profile of this emission band is similar to that obtained at room temperature except for reduced FWHM of the emission (0.38 eV). Under the excitation of 355 nm light, however, a shoulder appears on the high-energy side of the 645 nm emission band (for comparison, the 645 nm emission spectra acquired at 77 K and 300 K under 355 nm excitation are

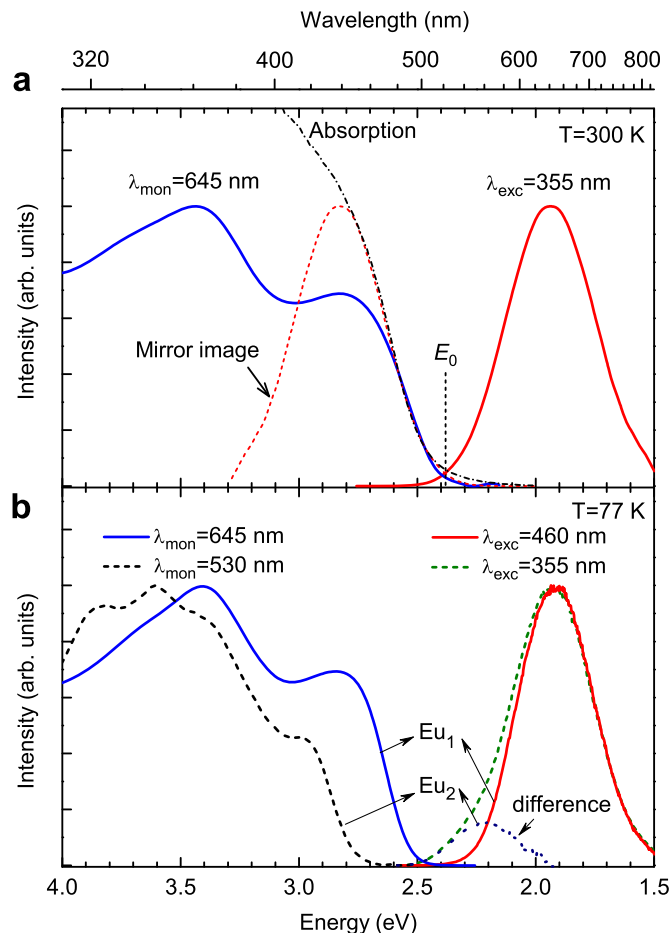


Figure 1 | PL emission and excitation spectra of *h*-EAO phosphor. (a), Emission (red), excitation (blue), and diffuse reflectance absorption spectra of *h*-EAO phosphor acquired at room temperature. The dashed line curve represents the “mirror image” reflection of the emission spectrum about the zero-phonon line energy E_0 . (b), Normalized emission and excitation spectra of *h*-EAO acquired at 77 K. The difference between the emission spectra excited by 355 nm and 460 nm is represented by an additional emission band peaked at 550 nm.

re-displayed in Supplementary Fig. 2b). The difference between the normalized emission spectra excited under 355 nm and 460 nm light is represented by an additional small band peaked at 550 nm (Fig. 1b). Moreover, at 77 K, the excitation spectrum obtained while monitoring the high-energy emission shoulder (e.g., at 530 nm; by selecting this wavelength we can monitor the 550 nm emission band and avoid the overlap with the 645 nm band) shifts to a shorter wavelength than the excitation spectrum of the 645 nm emission (Fig. 1b). Both the emission and excitation spectra suggest the existence of two different Eu^{2+} luminescent sites in *h*-EAO. We call them Eu_1 site and Eu_2 site, and they are responsible for the 645 nm and 550 nm broadband emissions at 77 K, respectively, as indicated in Fig. 1b.

Spectral identification of two Eu^{2+} luminescent sites. To confirm the presence of two Eu^{2+} sites in *h*-EAO, we measured wavelength dependent luminescence decays under the excitation of a 355 nm pulsed laser at 77 K. A set of luminescence decay curves were recorded at 77 K by monitoring emission wavelengths between 550–690 nm in 10 nm steps (Supplementary Fig. 3). Under the assumption that there exist two Eu^{2+} sites, we fitted the decay curves using a double exponential formula $I(t, \lambda) = A_1(\lambda) \times \exp(-t/\tau_1) + A_2(\lambda) \times \exp(-t/\tau_2)$, where $I(t, \lambda)$ represents the total



emission intensity at time t after the excitation pulse and at the monitoring wavelength λ ; $A_1(\lambda)$ and $A_2(\lambda)$ are the fractional PL emission intensities contributed by Eu_1 site and Eu_2 site, respectively, at the monitoring wavelength λ ; τ_1 and τ_2 are the luminescence lifetimes of Eu_1 site and Eu_2 site, respectively. It is expected that once the lifetimes τ_1 and τ_2 are determined, the existence of Eu_1 site and Eu_2 site can then be confirmed. At the same time, the PL spectral contributions from the two sites can be determined using the $A_2(\lambda)/A_1(\lambda)$ ratios. Our fitting results showed that the luminescence decay curves monitored between 630–690 nm can be well reproduced by a series of monoexponential functions (i.e., $A_2(630\text{--}690) = 0$) with the fitted lifetime $\tau_1 = 1.27 \mu\text{s}$ (Supplementary Fig. 3). As an example, the decay curve monitored at 650 nm and its fitted profile are given in Fig. 2a. In contrast to the monoexponential decay curves obtained between 630–690 nm, the decay curves monitored between 550–620 nm can be well reproduced by a series of double-exponential functions with the fitted lifetime $\tau_2 = 0.57 \mu\text{s}$ and a fixed τ_1 ($1.27 \mu\text{s}$) (Supplementary Fig. 3). The $A_1(550\text{--}620)$ and $A_2(550\text{--}620)$ values were obtained in the same fitting. As an example, the decay curve monitored at 550 nm and its fitted profile are also shown in Fig. 2a. The $A_2(\lambda)/A_1(\lambda)$ ratios are then plotted as a function of emission wavelengths (550–690 nm) in Fig. 2b (solid ball curve), along with the emission spectra from the two sites at 77 K. The monoexponential decay behavior ($A_2/A_1 = 0$) between 630–690 nm is consistent with the absence of the emission from the Eu_2 site in this long-wavelength emission region (Fig. 2b). In the range of 550–620 nm, the A_2/A_1 value increases as the wavelength decreases, which corresponds to the increase of the 550 nm emission contribution and the decrease of the 645 nm emission contribution; this verifies the existence of the additional 550 nm emission band from Eu_2 site at 77 K.

We attribute the 550 nm emission band and its corresponding excitation spectrum at 77 K (Fig. 1b) to the $4f^{65d} \leftrightarrow 4f^7$ transitions of the Eu^{2+} luminescent center (Eu_2 site) due to the spectral similarity between the current spectra and the reported spectra of Eu^{2+} -activated green aluminate phosphors³. However, the lifetime of the 550 nm emission (τ_2 , $0.57 \mu\text{s}$) is much shorter than the typical radiative lifetimes of the green emissions from the Eu^{2+} -activated green aluminate phosphors ($\sim 1.2 \mu\text{s}$)¹⁷. This can occur because the 550 nm emission from Eu_2 site might be partially quenched by the

energy transfer between Eu_2 site and Eu_1 site even at 77 K. That is, the lifetime of $0.57 \mu\text{s}$ at 77 K may not represent the radiative lifetime of Eu_2 site. Indeed, the small spectral overlap between the 550 nm emission band (Eu_2 site) and the 435 nm excitation band (Eu_1 site) at 77 K (Fig. 1) makes it possible for the energy transfer to occur from the Eu_2 site to the Eu_1 site. Moreover, the decay curve monitored at 650 nm (Eu_1 site only) exhibits a build-up at the initial decay stage ($0.34\text{--}0.46 \mu\text{s}$, the shaded area in the inset of Fig. 2a), while during that same time period the decay curve monitored at 550 nm (dominated by Eu_2 site) exhibits a faster decay. The different initial decays at the 650 nm and 550 nm emissions provide unambiguous evidence for energy transfer from the Eu_2 site to the Eu_1 site. At higher temperature, e.g., room temperature, more efficient energy transfer from the high-energy Eu_2 site to the low-energy Eu_1 site is expected due to the stronger spectral overlap. Thus, the energy transfer can cause the complete quenching of the 550 nm emission band at room temperature (Fig. 1a).

Localized/delocalized characters of the 645 nm emitting state. The above results reveal that the 645 nm emission band from the Eu_1 site is the dominant emission band at 77 K and the only emission band at room temperature. The nature of the emitting state corresponding to the 645 nm emission band can be initially revealed by its radiative lifetime whose value ($1.27 \mu\text{s}$) is close to the typical value ($\sim 1.1 \mu\text{s}$) of the normal $\text{Eu}^{2+} 4f^{65d} \rightarrow 4f^7$ emission in solids¹⁷. This indicates that the wave function of the emitting state (i.e., the lowest excited state) should contain dominant $4f^{65d}$ compositions. Meanwhile, the presence of a distinct PL excitation band at 435 nm indicates that there is a large transition moment between the $4f^7$ ground state and the lowest excited state, which further confirms the dominant $4f^{65d}$ character of the emitting state¹⁸. Thus, the 645 nm emission may originate from the lowest $4f^{65d}$ level of Eu^{2+} luminescent center (Eu_1 site) whose eigenfunction is a localized $4f^{65d}$ composition. However, both the FWHM (0.38 eV at 77 K and 0.45 eV at room temperature) and the Stokes shift (0.92 eV) of the 645 nm emission are significantly larger than those reported previously in Eu^{2+} -activated aluminate phosphors³. These extraordinarily large values suggest that the 645 nm broadband emission is uncharacteristic of the normal $\text{Eu}^{2+} 4f^{65d} \rightarrow 4f^7$ transition. Based on the above discussion, we deduce that the emitting state corresponding to the

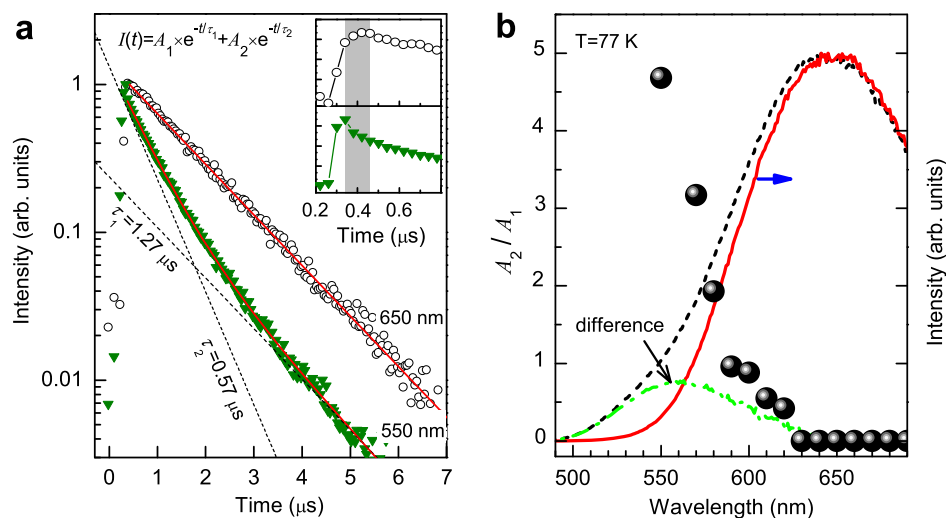


Figure 2 | Spectral identification of Eu^{2+} luminescent sites in h -EAO. (a), Normalized luminescence decay curves of h -EAO monitored at 650 nm and 550 nm emissions at 77 K. The excitation source is a 355 nm Nd:YAG pulsed laser. The red solid lines are the fitted profiles. The black dashed lines are the decomposed decay compositions. Inset is a zoomed-in view of the initial stage of the decays for the two emission wavelengths. (b), Plot of PL spectral distribution (A_2/A_1) over two Eu^{2+} sites (Eu_1 and Eu_2) as a function of emission wavelengths at 77 K (solid balls). The line curves are the PL emission spectra from Eu_1 and Eu_2 sites at 77 K, which are the same as the emission curves in Fig. 1b.

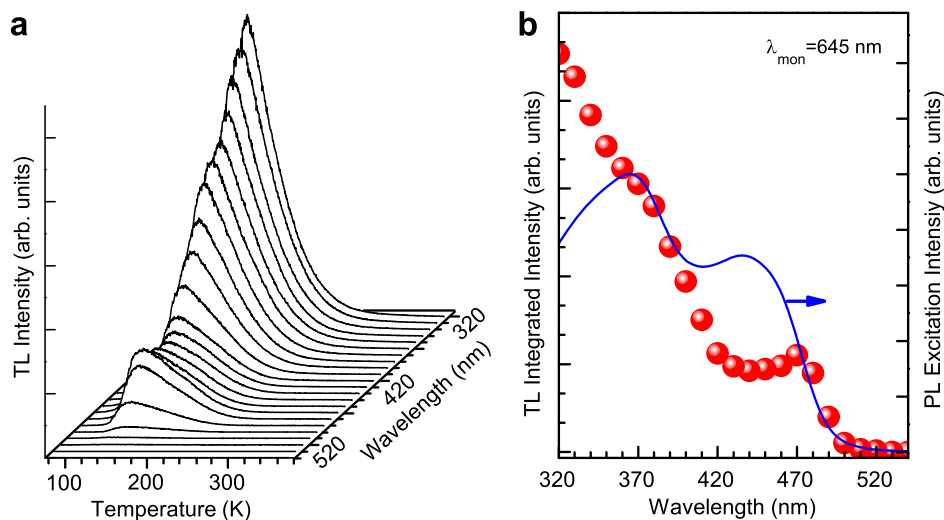


Figure 3 | TL excitation spectroscopy measurements of *h*-EAO. (a), TL curves of *h*-EAO monitored at 645 nm emission. The sample was illuminated with 320–540 nm light in 10 nm steps for 10 min at 77 K. The measured temperature varied from 77 to 380 K. (b), TL integrated intensities as a function of excitation wavelengths (red balls). The solid line curve is the PL excitation spectrum of *h*-EAO monitored at 645 nm emission at 77 K, which is the same as the blue line curve in Fig. 1b.

645 nm emission band is essentially a $4f^{65d}$ composition but probably not a normal localized state.

To further understand the unusual 645 nm emission, we conducted photoionization experiments based on thermoluminescence (TL) excitation spectroscopy. The measurements were carried out by illuminating *h*-EAO at 77 K for 10 min with monochromatic light whose wavelength was tuned between 320–540 nm in 10 nm steps. If the excitation energy is high enough to promote the $4f^7$ ground state electron to a delocalized state, the delocalized electron possibly will be captured by electron traps (such as disordered oxygen vacancies, which are inevitably created in reducing synthesis environment¹⁹) at 77 K and subsequently released during heating, followed by the recombination with the ionized luminescent center. Figure 3a shows a set of TL curves monitored at 645 nm; each was recorded from 77 to 380 K at a linear heating rate of 4 K/s. These TL curves show similar spectral shapes but with varied TL intensities. A typical TL spectrum contains an asymmetric broadband ranging from 90 to 290 K and peaking at ~ 135 K, indicating that the traps are distributed over a wide range of energies below the host conduction band in *h*-EAO. According to previous studies^{20–22}, the delocalization energy of the excited electron at 77 K can be determined from the TL creation spectrum, i.e., the plot of TL integrated intensities versus the illumination wavelengths, as shown by the red ball curve in Fig. 3b (Note that the effect of thermally activated ionization is eliminated at 77 K). For comparison, the PL excitation spectrum at 77 K monitoring the 645 nm emission is also presented. Figure 3b shows that the onset of the electron delocalization energy coincides with the onset of the lowest PL excitation energy at ~ 500 nm, revealing the delocalized character of the lowest excited state of the Eu_1 site at 77 K. Taking the luminescence performances of Eu_1 site into account, the optical excitation of the lowest excited state in *h*-EAO at 77 K should be followed by an autoionization process¹⁸. This means that the lowest excited state (i.e. the emitting state) is a mixed state consisting of dominant localized $4f^{65d}$ states and complementary delocalized conduction-band-like states. In other words, the 645 nm emitting state acquires some properties of the delocalized state, opening the channels for electron delocalization from the Eu^{2+} luminescent center.

Discussion

The autoionization-associated $4f^{65d}$ emitting state proposed here is different from either the localized $4f^{65d}$ state of the normal

$4f^{65d} \rightarrow 4f^7$ transition or the delocalized exciton-like state of anomalous luminescence. As a result of electron delocalization in the emitting state, the ligand ions around the luminescent center (i.e., Eu_1 site) will undergo a considerable relaxation, which is reflected in the emission spectrum by an extraordinarily large FWHM and an extremely large Stokes shift in *h*-EAO. Besides the energy threshold at ~ 500 nm, the TL creation spectrum in Fig. 3b also contains a higher energy threshold at ~ 420 nm. The strong electron delocalization in the high-energy region (i.e., 320–420 nm) can be attributed to the autoionizing intermediate states, i.e., the autoionization of $4f^{65d}$ states lying in the host conduction band^{20–22}.

We have carried out a detailed study on a new hexagonal EuAl_2O_4 phosphor whose Eu^{2+} luminescence exhibits a very large bandwidth and an extremely large Stokes shift. At 77 K, two luminescent sites responsible for 645 nm and 550 nm broadband emissions were identified, while at room temperature, the 550 nm emission band was quenched due to energy transfer. The 645 nm emission exhibits both characteristic and uncharacteristic properties of a normal Eu^{2+} $4f^{65d} \rightarrow 4f^7$ transition, evidenced by a typical Eu^{2+} lifetime of 1.27 μs and an extremely large Stokes shift of 0.92 eV, respectively. Photoionization experiments showed that the emitting state of the 645 nm emission is a mixed state consisting of dominant localized $4f^{65d}$ states and complementary delocalized conduction-band-like states.

Methods

The optical properties of the *h*-EAO phosphor were studied using an array of spectral methods. The PL spectra were recorded using a FluoroLog-3 spectrofluorometer equipped with a 450-W xenon arc lamp as the excitation source. The diffuse reflectance absorption was measured using a Shimadzu UV-2450 UV-Vis spectrometer. The luminescence lifetime was recorded using a photomultiplier tube and a digital oscilloscope under excitation with the third harmonic (355 nm) of a Nd:YAG pulsed laser. The TL curves were recorded using the FluoroLog-3 spectrofluorometer and a homemade TL setup. Appropriate optical filters were used to avoid stray light in all optical measurements.

- Blasse, G., Wanmaker, W. L., ter Vrugt, J. W. & Bril, A. Fluorescence of Eu^{2+} -activated silicates. *Philips Res. Rep.* **23**, 189–200 (1968).
- Poort, S. H. M. & Blasse, G. The influence of the host lattice on the luminescence of divalent europium. *J. Lumin.* **72–74**, 247–249 (1997).
- Dorenbos, P. Energy of the first $4f^7 \rightarrow 4f^{65d}$ transition of Eu^{2+} in inorganic compounds. *J. Lumin.* **104**, 239–260 (2003).
- McClure, D. S. & Pédrini, C. Excitons trapped at impurity centers in highly ionic crystals. *Phys. Rev. B* **32**, 8465–8468 (1985).



5. Moine, B., Pédrini, C. & Courtois, B. Photoionization and luminescences in $\text{BaF}_2:\text{Eu}^{2+}$. *J. Lumin.* **50**, 31–38 (1991).
6. Dorenbos, P. Anomalous luminescence of Eu^{2+} and Yb^{3+} in inorganic compounds. *J. Phys.: Condens. Mater.* **15**, 2645–2665 (2003).
7. Swiatek, K., Godlewski, M. & Hommel, D. Deep europium-bound exciton in a ZnS lattice. *Phys. Rev. B* **42**, 3628–3633 (1990).
8. Gatch, D. B. *et al.* Pressure dependence of the impurity-trapped exciton emission in $\text{BaF}_2:\text{Eu}$ and $\text{Ba}_x\text{Sr}_{1-x}\text{F}_2:\text{Eu}$. *Phys. Rev. B* **74**, 195117 (2006).
9. Smet, P. F. *et al.* Anomalous photoluminescence in $\text{BaS}:\text{Eu}$. *Phys. Rev. B* **74**, 035207 (2006).
10. Poort, S. H. M., Blokpoel, W. P. & Blasse, G. Luminescence of Eu^{2+} in barium and strontium aluminate and gallate. *Chem. Mater.* **7**, 1547–1551 (1995).
11. Tang, Y. S. *et al.* Near-ultraviolet excitable orange-yellow $\text{Sr}_3(\text{Al}_2\text{O}_5)\text{Cl}_2:\text{Eu}^{2+}$ phosphor for potential application in light-emitting diodes. *Appl. Phys. Lett.* **93**, 131114 (2008).
12. Srivastava, A. M. *et al.* Unusual luminescence of octahedrally coordinated divalent europium ion in $\text{Cs}_2\text{M}^{2+}\text{P}_2\text{O}_7$ ($\text{M}^{2+} = \text{Ca}, \text{Sr}$). *J. Lumin.* **129**, 919–926 (2009).
13. Krings, M., Montana, G., Dronskowski, R. & Wickleder, R. $\alpha\text{-SrNCN}:\text{Eu}^{2+}$ – a novel efficient orange-emitting phosphor. *Chem. Mater.* **23**, 1694–1699 (2011).
14. Daicho, H. *et al.* A novel phosphor for glareless white light-emitting diodes. *Nat. Commun.* **3**, 1132 (2012).
15. Li, X. F. *et al.* New yellow $\text{Ba}_{0.93}\text{Eu}_{0.07}\text{Al}_2\text{O}_4$ phosphor for warm-white light-emitting diodes through single-emitting-center conversion. *Light: Sci. Appl.* **2**, e50 (2013).
16. Liu, F. *et al.* New ternary europium aluminate luminescent nanoribbons for advanced photonics. *Adv. Funct. Mater.* **23**, 1998–2006 (2013).
17. Poort, S. H. M., Meijerink, A. & Blasse, G. Lifetime measurements in Eu^{2+} -doped host lattices. *J. Phys. Chem. Solids* **58**, 1451–1456 (1997).
18. Pédrini, C., Joubert, M. F. & McClure, D. S. Photoionization processes of rare-earth dopant ions in ionic crystals. *J. Lumin.* **125**, 230–237 (2007).
19. Schierning, G., Batentschuk, M., Osvet, A., Stiegelschmitt, A. & Winnacker, A. The influence of lattice defects on fluorescence and phosphorescence in the europium aluminate EuAl_2O_4 . *Phys. Stat. Sol. (C)* **2**, 109–112 (2005).
20. Fleniken, J., Wang, J., Grimm, J., Weber, M. J. & Happek, U. Thermally stimulated luminescence excitation spectroscopy (TSLES): a versatile technique to study electron transfer processes in solids. *J. Lumin.* **94–95**, 465–469 (2001).
21. van der Kolk, E., de Haas, J. T. M., Bos, A. J. J., van Eijk, C. W. E. & Dorenbos, P. Luminescence quenching by photoionization and electron transport in a $\text{LaAlO}_3:\text{Ce}^{3+}$ crystal. *J. Appl. Phys.* **101**, 083703 (2007).
22. You, F. T., Bos, A. J. J., Shi, Q. F., Huang, S. H. & Dorenbos, P. Thermoluminescence investigation of donor (Ce^{3+} , Pr^{3+} , Tb^{3+}) acceptor (Eu^{3+} , Yb^{3+}) pairs in $\text{Y}_3\text{Al}_5\text{O}_{12}$. *Phys. Rev. B* **85**, 115101 (2012).

Acknowledgments

Z.W.P. acknowledges the funding support from the US National Science Foundation (NSF DMR-0955908). J.D.B. was supported by the Materials Sciences and Engineering Division, Office of Basic Energy Sciences, U.S. Department of Energy (DOE). Use of the Advanced Photon Source 15-ID ChemMatCARS facility was supported by U.S. DOE under Contract No. DE-AC02-06CH11357 with Argonne National Laboratory. ChemMatCARS Sector 15 is principally supported by the Divisions of Chemistry and Materials Research, NSF, under grant number NSF/CHE-1346572.

Author contributions

Z.W.P. and F.L. conceived the study and wrote the paper. F.L. synthesized the material. F.L. and X.F.L. carried out spectral measurements. F.L., R.S.M. and Z.W.P. investigated the luminescence mechanism. J.D.B. and Y.S.C. carried out crystallographic measurements and analysis. All authors discussed the results and commented on the manuscript.

Additional information

Supplementary information accompanies this paper at <http://www.nature.com/scientificreports>

Competing financial interests: The authors declare no competing financial interests.

How to cite this article: Liu, F. *et al.* New localized/delocalized emitting state of Eu^{2+} in orange-emitting hexagonal EuAl_2O_4 . *Sci. Rep.* **4**, 7101; DOI:10.1038/srep07101 (2014).



This work is licensed under a Creative Commons Attribution-NonCommercial-NoDerivs 4.0 International License. The images or other third party material in this article are included in the article's Creative Commons license, unless indicated otherwise in the credit line; if the material is not included under the Creative Commons license, users will need to obtain permission from the license holder in order to reproduce the material. To view a copy of this license, visit <http://creativecommons.org/licenses/by-nc-nd/4.0/>